Hindawi
Shock and Vibration
Volume 2020, Article ID 8817631, 14 pages
https://doi.org/10.1155/2020/8817631

Research Article

Development of a Model to Predict Vibrations Induced by Blasting Excavation of Deep Rock Masses under High In Situ Stress

Yong Fan,[1,2] **Xianze Cui**,[1] **Zhendong Leng**,[1,3] **Yurong Zhou**,[1] **Junwei Zheng**,[1] **and Feng Wang**[1]

[1]*Hubei Key Laboratory of Construction and Management in Hydropower Engineering, China Three Gorges University, Yichang 443002, China*
[2]*Key Laboratory of Rock Mechanics in Hydraulic Structural Engineering, Ministry of Education, Wuhan University, Wuhan 430072, Hubei, China*
[3]*China Gezhouba Group Explosive Co. Ltd., Chongqing 401121, China*

Correspondence should be addressed to Junwei Zheng; jjunweizheng@163.com

Received 1 July 2020; Revised 12 October 2020; Accepted 21 October 2020; Published 2 November 2020

Academic Editor: Mohamed Abdelkareem

During the process of blasting excavation of deep rock masses under high in situ stress, energy produced by the explosive and the strain energy released by rock mass excavation constitute the energy source of vibration. However, in traditional Sadov's empirical formula, the energy produced by explosive explosion is only considered which makes the error higher when it is used to predict the blasting-induced vibration peak under the condition of high in situ stress. In this study, energy transformation and distribution mechanisms caused by excavation of deep rock masses were analyzed at first. Then, a prediction model of vibration peak based on the principle of energy balance was established by dimension analysis. Finally, the proposed model was trained and tested with the vibration data monitored during the blasting excavation of deep buried tunnel in Jinping II hydropower station. The result shows that compared with the traditional prediction model, the proposed model has higher fitting correlation coefficient and lower root-mean-square error, which can be better applied to the prediction of vibration induced by blasting excavation of deep rock masses under high in situ stress.

1. Introduction

As a clean energy, water energy is characterized by sustainable utilization. In the way of water energy utilization, hydropower technology is relatively mature, and it is regarded as the first choice for development all over the world. In order to make full use of hydropower advantages in western China, a great deal of large-scale hydropower projects including Lianghekou, Wudongde, and Baihetan are being or will be carried out in the southwest region [1]. Restricted by the canyon topography in southwest China, most of these projects need to place hydraulic structures underground, and all of them are characterized by large burial depth and high in situ stress during construction. For instance, the Jinping II hydropower station located in Yalong River bend has four diversion tunnels with a general buried depth of 1500–2000 m, a maximum buried depth of 2525 m, and a maximum principal stress of 70 MPa [2, 3]. When excavating the large-scale underground caverns under high in situ stress condition, the drilling and blasting method is often adopted. During drilling and blasting excavation, with the detonation of blast holes on the excavation face, the shock wave and stress wave produced by explosive explosion causes vibration in the retained rock masses. Moreover, when the vibration amplitude caused by excavation exceeds the safety threshold, it will inevitably produce adverse effects on the excavation tunnel itself or adjacent hydraulic structures, thus leading to a series of engineering geological disasters such as surrounding rock damage, surrounding rock deformation, rockbursts, and structure damage. Therefore, the vibration induced by tunnel blasting excavation in surrounding rock masses under the condition

of large buried depth and medium-high in situ stress becomes the key problem affecting the stability of surrounding rock, threatening the construction security of underground engineering, and causing geological disasters to slow down the construction progress.

A scientific and accurate dynamic model and calculation method often play an important role in the investigation of vibration regularity caused by underground blasting excavation of surrounding rock masses. Using the meshfree particle method, Rabczuk [4–6] presented innovative approaches for blast loading-driven fracture accounting for fluid-structure interaction, which provides a significantly new insight for the study of rock mass cracking, crack propagation, and vibration in retained rock mass under the action of shock wave and stress wave produced by explosive explosion during underground blasting excavation. In addition, a number of researchers have investigated the attenuation regularity of blasting vibration combined with a field test, theoretical calculation, and numerical simulation and proposed and improved the blasting vibration prediction model [7–13]. In current engineering application, Sadov's empirical formula is generally employed to investigate the association of blasting-induced vibration and blasting center distance and charging amount [14–17]. This formula reflects the influence of the explosive as an energy source on blasting vibration, which can be used to predict vibration in surface blasting. However, for deep rock blasting excavation under a high in situ stress condition, besides the explosion energy, the strain energy released by the rock mass during blasting excavation is also the energy source of vibration [18–20]. Moreover, as early as 1972, Toksöz and Kehrer [21] found that underground nuclear explosion can lead to rapid release of energy in deep rock masses, thus inducing artificial vibration, and the amplitude of artificial vibration may exceed that of nuclear explosion. For the case of high in situ stress, not only the energy release of rock mass and explosive play a controlling role in the whole vibration but also the in situ stress is an important influencing factor, in which the direction of in situ stress has a significant impact on the vibration propagation direction [22, 23]. Furthermore, in the direction of the maximum principal in situ stress, the peak value of vibration velocity of surrounding rock masses caused by blasting unloading is the greatest, and the influence of the in situ stress field on the middle and far region of the blasting source is more significant than that in the nearby region of the blasting source [24, 25]. Similarly, Lu et al. [18–20] further reported that the surrounding rock vibration produced during blasting excavation of deep rock mass is the superposition of the vibration derived from explosion load and the vibration caused by transient stress unloading induced energy release of the surrounding rock mass, and the vibration induced by energy release of the rock mass may exceed the vibration produced by explosion load and become the main component of surrounding rock vibration. The studies mentioned above fully indicate that it is inaccurate to predict the peak value of blasting excavation-induced vibration in deep rock mass by using Sadov's empirical formula and its improved formula, which only consider the energy produced by explosive explosion and neglect the release of strain energy of the rock mass for the case of high in situ stress.

The purpose of this paper is to establish an accurate vibration peak prediction model by taking into account the strain energy release factor of deep rock masses. In this paper, based on the analysis of energy transformation and distribution law of deep rock mass excavation under high in situ stress condition, a prediction model of peak vibration induced by blasting excavation of deep rock mass was established using dimensional analysis. The rationality and correctness of the prediction model proposed in this paper were tested with the vibration data monitored during the blasting excavation of the deep buried tunnel in the Jinping II hydropower station.

2. Energy Source of Vibration Induced by Blasting Excavation of Deep Rock Masses

Large buried depth and high in situ stress endow the rock mass with high strain energy. During the blasting excavation of high energy-storage rock masses, with detonation of explosives in the blasting hole, the rock mass is broken and the fragment is thrown. The high strain energy of the rock mass imparted by the high in situ stress will be released quickly, and the vibration will be induced in surrounding rock masses which is superimposed with the vibration produced by the chemical energy released by explosives. Therefore, compared with vibration generated by the surface blasting, there are two energy sources for the vibration induced by the blasting of deep rock masses under high in situ stress: the chemical energy produced by explosive explosion and the strain energy released by rock masses. In order to predict the vibration induced by blasting excavation of deep rock masses under high in situ stress, the transformation and distribution mechanism of chemical energy produced by explosive explosion and the strain energy released by rock masses should be investigated first.

2.1. Chemical Energy Produced by Explosion. During the blasting excavation of deep rock masses, the chemical energy generated by explosive explosion converts into four parts: the energy used to break the rock masses E_f, the energy used to throw fragments E_k, the energy used to generate vibrations E_v, and the uncountable part E_r. This balance system of energy can be described by the following equation:

$$E_E = E_f + E_k + E_v + E_r, \tag{1}$$

where E_E is the total energy produced by explosive explosion which can be calculated by the following equation:

$$E_E = QW, \tag{2}$$

where W is the explosion heat of the explosive; Q is the single charge quantity. According to the spherical wave theory, Sanchidrian et al. [26] proposed the calculation method of vibration energy E_v in the middle and far distance from the explosion source, as shown in the following equation:

$$E_v = 4\pi r^2 \rho C_L \int_0^T v^2 \mathrm{d}t, \tag{3}$$

where v is the vibration velocity equal to the vector sum of the vibration velocity in radial, horizontal, and vertical directions; T is the duration time of vibration; r is the distance from the blasting center; ρ is the density of the rock mass; and C_L is the longitudinal wave velocity. Equation (3) can not only be used to calculate the energy of vibration produced by explosion load E_{vb} but also can be adopted to count the energy of vibration induced by excavation unloading E_{vt}.

According to equation (2) and equation (3), the energy efficiency of blasting vibration η can be defined by the following formula:

$$\eta = \frac{E_{vb}}{E_E} \times 100\%. \tag{4}$$

The vibration energy efficiency η can be calculated according to the explosion heat of the explosive W, the single charge quantity Q, and the vibration energy E_{vb} produced by explosive explosion.

2.2. Strain Energy Released by the Excavation of the Rock Masses. Considering that the rock mass with volume of V is excavated by drilling and blasting method under the high in situ stress, the stress constraint of the excavated rock mass acting on the retained rock mass releases instantaneously on the newly formed excavation surface (area of S). Thus, the transient unloading of in situ stress caused by blasting excavation will inevitably result in the energy change of surrounding rock masses, and the new energy system consists of four parts: the work done by the force on the outer boundary W_1; the increased strain energy in the rock mass J; the work done by the unreleased stress on the excavation surface W_2; and the energy released by the rock excavation (W_r). Therefore, the energy balance system can be described as follows:

$$W_1 - (J + W_2) = W_r. \tag{5}$$

If the surrounding rock mass is not damaged and still remain the homogeneous elastic medium after excavation, the energy W_r released by the rock mass excavation will be dissipated in the form of vibration. Assuming that the excavation of the rock mass is completed in an instant, the energy E_{vt} used to produce the vibration and the strain energy U of excavated rock masses can be calculated using equations (6) and (7), respectively.

$$E_{vt} = \frac{1}{2} \int_0^S \sigma_i^A u_i^B \mathrm{d}S, \tag{6}$$

$$U = \frac{1}{2} \int_0^S \sigma_i^A u_i^A \mathrm{d}S, \tag{7}$$

where σ_i is the in situ stress ($i = 1, 2, 3$), u_i is the displacement, A is the state before excavation, and B is the state after excavation. As can be seen from equations (6) and (7), in a particular working condition, the energy W_v used to cause the vibration in the energy released by the rock mass excavation is closely associated to the strain energy U of the excavated rock mass. However, as Salamon [27] demonstrated, this relationship could only be quantified when the shape of the excavated rock masses and the in situ stress are known.

Assuming that a spherical cave with radius of a is excavated in the deep rock mass under the condition of hydrostatic-compressive stress field ($\sigma_1 = \sigma_2 = \sigma_3 = P_0$), the secondary stress field and the displacement field of surrounding rock masses in the coordinate axis of the spherical coordinate system (r, θ, φ) after excavation are as follows:

$$\begin{aligned} \sigma_r &= P_0\left(1 - \frac{a^3}{r^3}\right), \\ \sigma_\theta &= \sigma_\varphi = P_0\left(1 + \frac{a^3}{2r^3}\right), \\ u_r &= \frac{P_0 a^3}{4Gr^2}, \end{aligned} \tag{8}$$

where σ_r, σ_θ, and σ_φ are the radial normal stress, annular normal stress, and tangential stress of surrounding rock masses after excavation, respectively; u_r is the radial displacement of the rock mass at radius of r; and G is the shear modulus, which is calculated by the following equation:

$$G = \frac{E_0}{2(1+\mu)}, \tag{9}$$

where E_0 is the elastic modulus of the rock mass and μ is the Poisson ratio of the rock mass.

The elastic strain energy of per unit volume of the rock mass or the strain energy density U_0 is calculated by the following equation:

$$U_0 = \frac{\left[\sigma_1^2 + \sigma_2^2 + \sigma_3^2 - 2\mu\left(\sigma_1\sigma_2 + \sigma_2\sigma_3 + \sigma_1\sigma_3\right)\right]}{2E_0}. \tag{10}$$

Before excavation, the rock mass is in the initial in situ stress state ($\sigma_1 = \sigma_2 = \sigma_3 = P_0$); then, the strain energy density of the rock mass before excavation U_y can be calculated by the following equation:

$$U_y = P_0^2 \frac{[3(1-2\mu)]}{2E_0}. \tag{11}$$

By substituting equation (8) into equation (11), the elastic strain energy density of the surrounding rock mass after excavation U_w can be obtained:

$$U_w = P_0^2 \frac{\left[\left(\left(3(1-2\mu) + 3(1+\mu)a^6\right)/2r^6\right)\right]}{2E_0}. \tag{12}$$

Then, the increment of strain energy density of the surrounding rock mass after excavation ΔU is

$$\Delta U = U_w - U_y = 3P_0^2 \frac{\left[\left((1+\mu)a^6\right)/r^6\right]}{4E_0}. \tag{13}$$

Combining equation (9), there are

$$\Delta U = \frac{3P_0^2 a^6}{8r^6 G}. \tag{14}$$

The work done by the distant surrounding rock mass (assuming that the radius r is large and set as $r_{+\infty}$) on the nearby surrounding rock mass W_1 is

$$W_1 = 4\pi a^2 \cdot P_0 \cdot u_r = 4\pi a^2 \cdot P_0 \cdot \frac{P_0 a^3}{4Ga^2} = \frac{\pi a^3 P_0^2}{G}. \tag{15}$$

Assuming that the vibration velocity of the particle on the excavation surface is $v(a,t)$, the radial stress on the excavation surface $P(t)$ is unloaded from $P(0)$ to 0 through the time of td, and the work W_2 done by the unreleased stress $P(t)$ is

$$W_2 = 4\pi a^2 \cdot \int_0^{t_d} P(t) \cdot v(a,t)\mathrm{d}t. \tag{16}$$

According to equation (14), the increment of strain energy of the surrounding rock mass in the nearby region J can be calculated by the following equation:

$$J = \int_a^{+\infty} 4\pi r^2 \Delta U \mathrm{d}r = \int_a^{+\infty} 4\pi r^2 \frac{3a^6 P_0^2}{8Gr^6}\mathrm{d}r = \frac{\pi a^3 P_0^2}{2G}. \tag{17}$$

The energy dissipated in the form of vibration W_r can be calculated by the following equation:

$$E_{vt} = W_r = \int_a^{r_{+\infty}} 4\pi r^2 \cdot \frac{1}{2}\rho v^2 \mathrm{d}r. \tag{18}$$

According to equation (5), the energy dissipated in the form of vibration W_r can also be calculated by the following equation:

$$E_{vt} = W_r = \frac{\pi a^3 P_0^2}{2G} - 4\pi a^2 \cdot \int_0^{t_d} P(t) \cdot v(a,t)\mathrm{d}t. \tag{19}$$

In the limiting case, if the unloading time $t_d = 0$, the work W_2 done by the unreleased stress $P(t)$ is equal to 0, and then, the energy dissipated in the form of vibration W_r is

$$E_{vt} = W_r = \frac{\pi a^3 P_0^2}{2G}. \tag{20}$$

According to equation (11), the total strain energy of the excavated rock mass U is

$$U = \frac{4}{3}\pi a^3 \cdot P_0^2 \frac{[3(1-2\mu)]}{2E_0} = \frac{2\pi a^3 P_0^2 (1-2\mu)}{E_0}. \tag{21}$$

It can be found from equations (20) and (21) that the energy E_{vt} released in the form of vibration is related to the total strain energy U of excavated rock masses, and the relationship is

$$E_{vt} = \frac{E_0}{4G(1-2\mu)} U. \tag{22}$$

If the in situ stress unloading on the excavated surface is completed within a few milliseconds, the energy E_{vt} released by rock masses in the form of vibration has the following relationship with the total strain energy U of the excavated rock mass:

$$E_{vt} = \left[\frac{E_0}{4G(1-2\mu)} - \frac{2E_0 \cdot \int_0^{t_d} P(t) \cdot v(a,t)\mathrm{d}t}{(1-2\mu)aP_0^2}\right] \cdot U = K_1 U, \tag{23}$$

where K_1 is the energy ratio of vibration caused by the stress unloading, and it is a constant related to the Poisson ratio, the elastic modulus, the unloading time of the in situ stress, and the unloading mode of the in situ stress.

The vibration caused by the chemical energy released by the explosive explosion and the vibration caused by strain energy release are superimposed, which constitutes the coupled vibration induced by the blasting excavation of the deep rock mass. Thus, the energy source of the coupled vibration includes two parts: one is the energy E_{vb} used to produce vibration by the explosive detonation, and the other is the energy E_{vt} released in the form of vibration, which is from the energy of the rock mass imparted by the high in situ stress, which can be calculated by the following equation:

$$E_t = E_{vb} + E_{vt} = \eta QW + K_1 U, \tag{24}$$

where E_t is the energy source of the coupled vibration caused by the blasting excavation of deep rock masses, which includes the energy released by the partial explosive explosion and the strain energy released by the excavation of rock masses.

3. Establishment of the Prediction Model

For the condition of a circular tunnel and the hydrostatic stress field, Lu and Hustrulid [28] proposed the equation of the vibration peak induced by the strain energy release of rock masses of the deep rock excavation in high in situ stress, which can describe the attenuation of vibration peak with the distance.

$$v = K_2 \frac{\overline{P}}{\rho C_p}\left(\frac{d}{r}\right)^{\lambda}, \tag{25}$$

where $\overline{P}$ is the in situ stress value on the excavation boundary (Pa); d is the unloading radius of excavation load (m); K_2 is the coefficient; and C_p is the elastic longitudinal wave velocity of the surrounding rock mass (m/s). The equation reflects the influence of the wave impedance of rock masses, the in situ stress value, and the unloading radius on the vibration induced by the strain energy release of the rock masses. However, it is difficult to use the equation under the conditions of irregular excavation boundary and the nonhydrostatic stress field.

Because equation (25) is based on the cylinder elastic wave theory, it is inaccurate to use this formula to analyze the attenuation law of transient stress unloading-induced vibration when the excavation boundary is irregular and the rock mass is under the nonhydrostatic stress field. Furthermore, according to the thermodynamic law, due to blasting excavation, the vibration induced by transient unloading is essentially a physical phenomenon driven by energy. Therefore, the influence of energy release of rock masses on vibration induced by blasting excavation cannot be ignored.

According to equation (23), the peak velocity of vibration induced by the release of strain energy (PPV) is closely associated to the strain energy of the excavated rock mass U, the excavation load $\overline{P}$, the volume of the excavated rock mass V, the elastic modulus E_0, the Poisson ratio μ, the rock mass density ρ, the longitudinal wave velocity C_L, the distance r, and other factors (when the blasting environment is known, the transient unloading time of the initial in situ stress on the excavation surface is a constant and it is not regarded), and the excavation load $\overline{P}$, the elastic modulus E_0, the Poisson ratio v, and the longitudinal wave velocity C_L can all be reflected in the strain energy of excavated rock mass U. Therefore, the physical quantities that affect the peak velocity of vibration (PPV) induced by the strain energy release include the strain energy of the excavated rock mass U, the volume of the excavated rock mass V, the rock mass density ρ, and the distance r. The coupled vibration caused by blasting excavation in deep rock mass is composed of the vibration caused by the strain energy release of the rock mass and the vibration caused by the explosive explosion. Combined with equation (24), the physical quantities that affect the coupled vibration induced by blasting excavation of the deep rock mass are the sum of energy generated by explosive explosion and the strain energy released by the rock excavation E_t, the volume of the excavated rock mass V, the distance from explosive source r, and the density of the rock mass ρ. These influencing factors can be described as

$$\mathrm{PPV} = F_1\left(E_t, V, \rho, r\right). \tag{26}$$

There are five physical quantities in equation. (26), and their dimensions are $[\mathrm{PPV}] = LT^{-1}$, $[E_t] = ML^2T^{-2}$, $[V] = L^3$, $[\rho] = ML^{-3}$, and $[r] = L$; among them, L, M, and T are the basic dimensions. According to π theorem, this physical quantity system can be described by two π equations:

$$\begin{aligned} \pi_1 &= E_t^{\alpha_1} V^{\beta_1} \rho^{\gamma_1} r, \\ \pi_2 &= E_t^{\alpha_1} V^{\beta_2} \rho^{\gamma_2} \mathrm{PPV}. \end{aligned} \tag{27}$$

Converting the physical quantities in equation (27) into the exponent of the basic dimension,

$$\begin{aligned} \pi_1 &= M^{\alpha_1+\gamma_1} \cdot L^{2\alpha_1+3\beta_1-3\gamma_1+1} \cdot T^{-2\alpha_1}, \\ \pi_2 &= M^{\alpha_2+\gamma_2} \cdot L^{2\alpha_2+3\beta_2-3\gamma_2+1} \cdot T^{-2\alpha_1-1}. \end{aligned} \tag{28}$$

Because π_1 and π_2 are dimensionless quantities, we can get

$$\begin{aligned} \alpha_1 + \gamma_1 &= 0, \\ 2\alpha_1 + 3\beta_1 - 3\gamma_1 + 1 &= 0, \\ -2\alpha_1 &= 0, \\ \alpha_2 + \gamma_2 &= 0, \\ 2\alpha_2 + 3\beta_2 - 3\gamma_2 + 1 &= 0, \\ -2\alpha_2 - 1 &= 0. \end{aligned} \tag{29}$$

By solving the abovementioned equations, $\alpha_1 = 0$, $\beta_1 = -1/3$, $\gamma_1 = 0$, $\pi_1 = r/V^{1/3}$, $\alpha_2 = -1/2$, $\beta_2 = 1/2$, $\gamma_2 = 1/2$, and $\pi_2 = \rho V/E_t^{1/2} \cdot \mathrm{PPV}$.

The function relation of dimensionless quantities can be expressed as

$$\left(\frac{\rho V}{E_t}\right)^{1/2} \cdot \mathrm{PPV} = F_2\left(\frac{r}{V^{1/3}}\right). \tag{30}$$

That is,

$$\mathrm{PPV} = \left(\frac{E_t}{\rho V}\right)^{1/2} F_2\left(\frac{r}{V^{1/3}}\right). \tag{31}$$

Since the peak velocity PPV of coupled vibration induced by blasting excavation of deep rock masses decreases gradually with the increase of distance r, the attenuation of the PPV can be described by the following equation:

$$\mathrm{PPV} = K_3\left(\frac{E_t}{\rho V}\right)^{1/2} \cdot \left(\frac{V^{1/3}}{r}\right)^{\beta}, \tag{32}$$

where K_3, β are unknown coefficients, which are obtained by the multiple regression method based on the data acquired from blasting tests, so as to accomplish the prediction of the vibration peak caused by the blasting excavation of the deep rock mass.

4. Engineering Applications

4.1. Project Background. The Jinping II hydropower station is located on the main stream of the Yalong River at the junction of Muli, Yanyuan, and Mianning counties in Liangshan Yi Autonomous Prefecture, Sichuan Province, China (Figure 1). It is a super large-scale underground diversion-type hydropower station under construction on the Yalong River, and it is also one of the backbone power stations of the west-east electricity transmission project. The hydropower station takes advantage of the 150 km natural drop of Yalong River bend to excavate tunnels and straightens the river bend to concentrate the water head for power generation, with the maximum head of 312 m and the rated head of 288 m. There are 8 mixed-flow hydrogenerators unit with a single capacity of 600 MW and a total installed capacity of 4800 MW installed in the power station. The hub of the power station is mainly composed of three parts: the head sluice, the water diversion system, and the underground powerhouse.

The water diversion system is arranged with 4 tunnels and 8 machines, with four parallel diversion tunnels crossing the Jinping Mountains. The azimuth of the main axis of the tunnel is N58°W, the center distance between the tunnels is 60 m, the length of the tunnel is about 16.67 km, the burial depth of the tunnels range 1500 to 2000 m, and the maximum burial depth is about 2525 m. While building the diversion tunnels, the maximum principal stress is nearly parallel to the axial of the tunnel in the direction of SE with a small dip angle, and its magnitude is around 1.1–1.3 times of the weight of the rock mass. The intermediate principal stress is nearly perpendicular to the axial of the tunnel in the direction of NE with a dip angle of 0 to 30°, and its magnitude is 1.0–1.2 times of the weight of the rock mass. The minimum principal stress is also basically perpendicular to

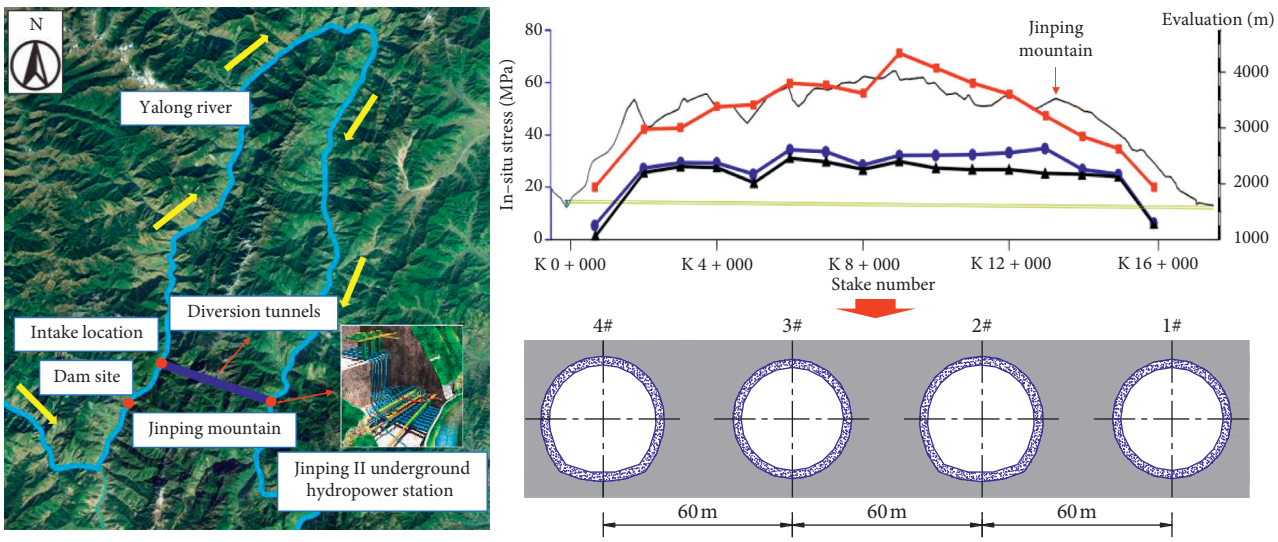

Figure 1: Layout of the Jinping II diversion tunnels.

the axial of the tunnel in the direction of SW with a larger dip angle of more than 60°, and its magnitude is 0.94–1.0 times of the rock mass. According to burial depth, the in situ stress level can be determined. Because the Jinping engineering area is the in situ stress concentrated area, the levels of in situ stress in the engineering area where the diversion tunnels located are high, and the inversion results show that the maximum principal stress of the diversion tunnel is about 72 MPa.

The four diversion tunnels were all excavated from the ends to the middle. Diversion tunnels #1 and #3 were constructed by the tunnel boring machine (TBM). The excavation section is circular with a diameter of 12.4 m, the total thickness of concrete lining is 60 cm, and the tunnel diameter after lining is 11.2 m. The diversion tunnels #2 and #4 were constructed by the drilling and blasting method, the excavated section is horseshoe-shaped and the diameter is 13.0 m, and the tunnel diameter after concrete lining is 11.8 m with the lining thickness of 40–60 cm. According to the working height of the trolley and the construction requirements of the bench construction and considering the difficulties in the one-time blasting excavation of the full section of the large-section tunnel with high in situ stress, the excavation sections of the diversion tunnels #2 and #4 were divided into an upper bench and lower bench for blasting excavation, and the upper bench and lower bench were constructed by the one-time blasting of the full section. Taking the blasting excavation of diversion tunnel #4 as an example, the excavation height of the upper bench is 8.0 m, the height of the lower bench is 5.0 m, the excavation footage is 4 m, and the blasting design is shown in Figure 2. The total number of blast holes is 209, the diameter of blast holes is 42 mm, the diameter of explosive rolls is 32 mm, the linear charge density of cut holes and break holes is 1.00 kg/m, and the charge of single blast hole is 4.0 kg. Interval charging was adopted for perimeter holes and bottom holes, the linear charge densities of them are 0.30 kg/m and 0.60 kg/m, respectively, and the charges of a single blast hole of them are 1.1 kg and 2.2 kg, respectively. The leyner cut was adopted for the cut blasting, and the smooth blasting was used for the contour excavation. During blasting, the $\varphi 32$ emulsion explosive was used. The upper bench and lower bench adopted the nonelectric millisecond delay detonator, which was divided into 16 sections for detonation, and the numbers in Figure 2 are the delay of explosives.

Vibration monitoring was carried out for a certain blasting of the upper bench in the diversion tunnel #4, and the vibration detector was arranged in the rock mass of the tunnel wall behind the tunnel face. The distances between the three monitoring points and the tunnel face are 15 m, 25 m, and 35 m, respectively, as shown in Figure 3. The time-history curves of the monitored vibration by monitoring points #2 and #3 are shown in Figure 4.

4.2. Characteristics of the Monitored Vibration Spectrum. If the surrounding rock mass during a certain blasting is regarded as a system, the energy produced by the explosive explosion and the strain energy released by the rock mass caused by excavation unloading are both the energy sources of the surrounding rock vibration, and the energy input of different mechanisms will inevitably cause the abrupt changes in the system energy. In the recent years, wavelet transform was widely used in signal processing because it can accomplish the abrupt change characteristics of signal energy.

The basic wavelet is supposed as $\psi(t)$, and then, the Moyal inner product theorem is used for the continuous wavelet transform of any energy-limited function $f(t)$ with respect to $\psi(t)$. The following equation holds:

$$\frac{1}{C_\psi}\int_R \frac{\mathrm{d}a}{a^2}\int_R \left|W_f(a,b)\right|^2 \mathrm{d}b = \int_R |f(t)|^2 \mathrm{d}t. \tag{33}$$

According to the energy density concept, equation (33) can be rewritten as

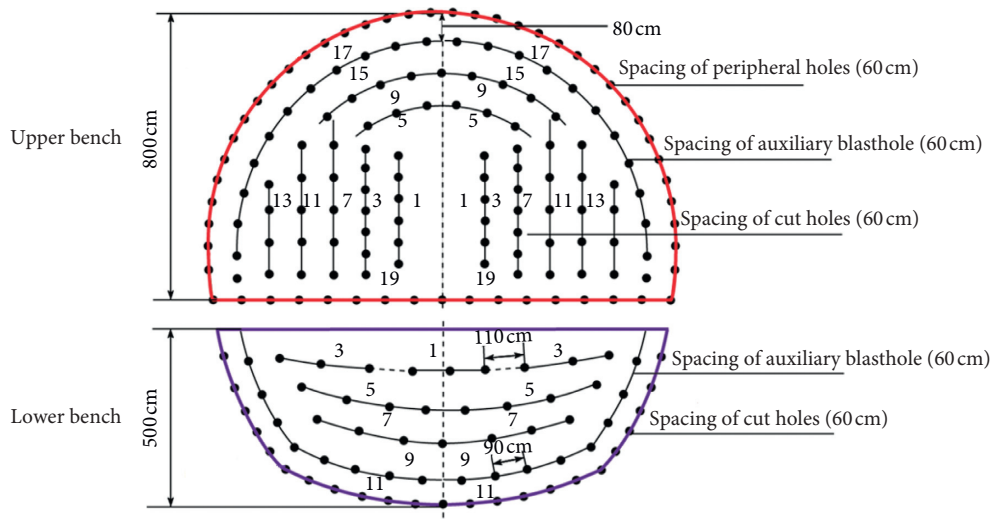

Figure 2: Blasting design of diversion tunnel #4 in the Jinping II hydropower station.

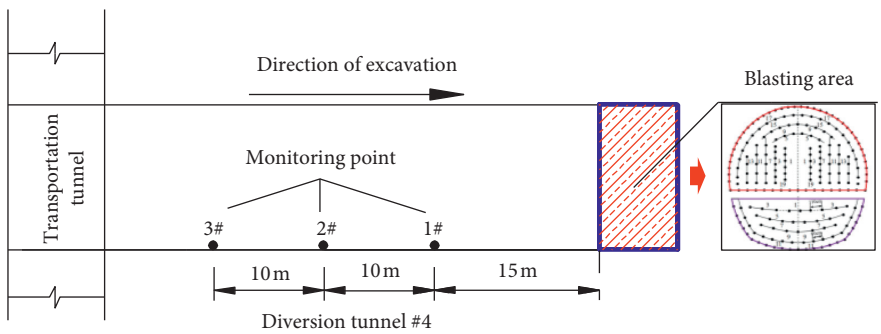

Figure 3: Layout of blasting vibration monitoring of diversion tunnel #4 for the Jinping II hydropower station.

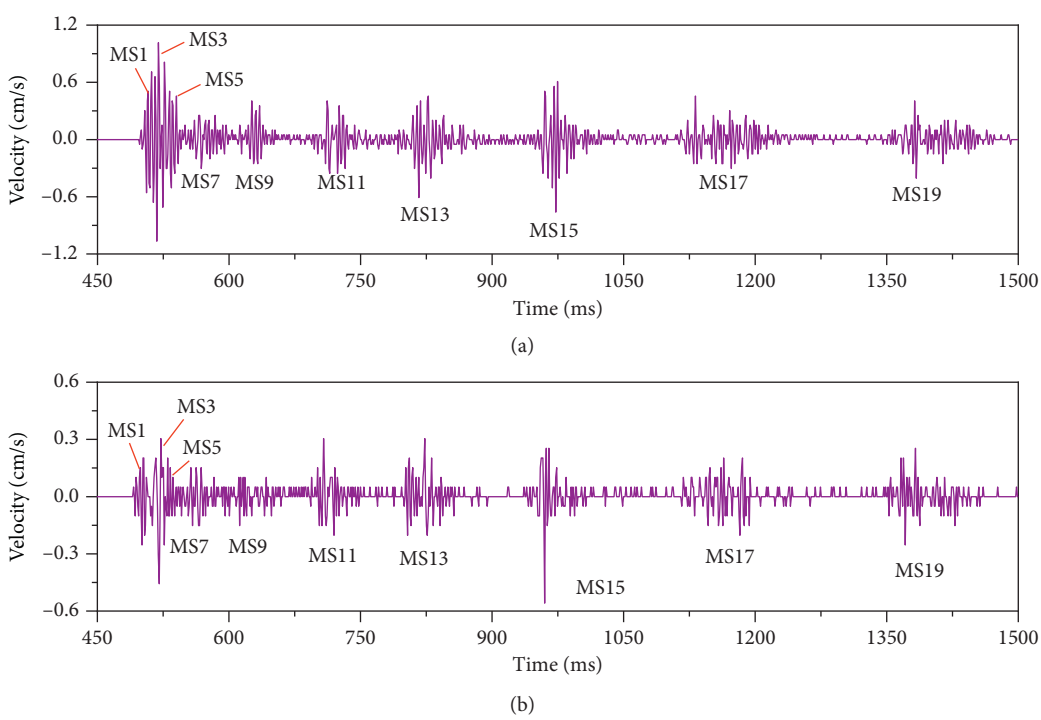

Figure 4: Time-history curves of the vertical vibration monitored during the blasting excavation of diversion tunnel #4 for the Jinping II hydropower station (monitoring points #2 and #3). (a) Monitoring point #2. (b) Monitoring point #3.

$$\int_R |f(t)|^2 \mathrm{d}t = \int_R E(b)\mathrm{d}b, \tag{34}$$

where

$$E(b) = \frac{1}{C_\psi}\int_R \frac{1}{a^2}\left|W_f(a,b)\right|^2 \mathrm{d}a. \tag{35}$$

In the wavelet transform, the scale a corresponds to the frequency ω. Thus, according to equation (35), the distribution of all frequency band energy of the signal over the time b can be obtained. If there are two excitation sources in a certain waveform, which are the explosive explosion and the strain energy transient release, and both of them will cause the abrupt change of the system energy. In this paper, the time-energy density analysis was carried out for the monitored vibration signal in Figure 4. Taking the monitored vibration waveforms of MS13 for monitoring points #2 and #3 as examples, the analysis results are shown in Figure 5. As can be seen from Figure 5, there are two obvious peak groups in the time-energy density distribution histogram of monitored vibration of the deep rock mass during blasting excavation under the high in situ stress. These two peak groups correspond to two different energy sources, which are the energy released by explosive detonation and the energy released by excavation unloading of the rock mass, respectively.

For the time-velocity curve of blasting vibration recorded in the actual engineering, it is sometimes difficult to express it by the accurate mathematical function relation, and the monitored waveform is composed of a large number of continuous data, which is not conducive for the fast calculation of computer. To solve this problem, the approximate processing was carried out on the original recorded data, that is, discrete sampling and quantization, and a finite discrete sequence $\{X_n\}$ is formed by selecting a finite number of discrete sampling values $(X_0, X_1, X_2, \ldots, X_n)$ from the processed data, which can be quickly transformed by the Fourier transform.

Assuming a function that varies continuously with time and taking discrete sampling for it, the sample length is T, the sampling interval is Δt, and the number of sample is N; then, N different sampling values form a discrete sequence $\{X_m x(m\Delta t)\}[m = 0, 1, 2, \ldots, (N-1)]$.

The m-th sampling time is $m\Delta t$, and its value is $x(m\Delta t)$. The Fourier series of the function $x(t)$ in the time domain T can be obtained by accumulation, which is shown in the following equation:.

$$x(t) = \frac{a_0}{2} + \sum_{k=1}^{N/2} a_k \cos\frac{2km\pi t}{N} + \sum_{k=1}^{N/2-1} b_k \sin\frac{2km\pi t}{N}, \tag{36}$$

where the Fourier coefficients a_k and b_k can be calculated as follows:

$$\begin{aligned} a_k &= \frac{2}{N}\sum_{m=0}^{N-1} x_m \cos\frac{2km\pi}{N}, \\ b_k &= \frac{2}{N}\sum_{m=0}^{N-1} x_m \sin\frac{2km\pi}{N}. \end{aligned} \tag{37}$$

According to the abovementioned Fourier analysis theory and DFT algorithm, the fast Fourier transform toolbox function provided by software Matlab was adopted to conduct the spectrum analysis of the monitored vibration signal in Figure 4. Taking the monitored waveforms of MS11 and MS13 for monitoring points #2 and #3 in the vertical direction as examples, the results of amplitude spectrum analysis are shown in Figure 6. As can be seen from Figure 6, both the amplitude spectrum curves of the monitored vibration have two dominant frequency bands, and the dividing points of the dominant frequency bands are about 185 Hz. This indicates that the vibration of different frequency bands is caused by the explosion load and the in situ stress unloading. The rising time of the explosion load is short, and the variation gradient of the explosion load is large, while the unloading time of the in situ stress is relatively long, which leads to the vibration signal of surrounding rock masses caused by in situ stress unloading contain more low-frequency energy. Therefore, the low-frequency band of the coupled vibration signal in Figure 6 is mainly caused by the in situ stress unloading, and the high-frequency band is mainly caused by the explosion load.

4.3. Training of the Prediction Model. In this paper, the Hanning window was adopted and the function of Matlab's signal processing toolbox was employed to design the FIR low-pass filter. According to the dividing point (185 Hz) of the dominant frequency band in the amplitude spectrum of the monitored vibration, the low-frequency signals are separated from the monitored vibration to obtain the time-history curve of vibration induced by the energy release of the rock mass during the excavation unloading process. Then, by subtracting the vibration waveform induced by the energy release from the original monitored vibration waveform, the vibration waveform caused by the explosive detonation can be obtained, which is as shown in Figure 7.

Squaring the vibration velocity in Figure 7 and integrating it with the abscissa, the energy of the vertical vibration can be obtained by equation (3). Then, by algebraically summing the energy of the vertical vibration with the energy of longitudinal vibration and the energy of horizontal tangential vibration, the vibration energy generated by the explosion load during the detonation of per delay and the vibration energy caused by the excavation unloading can be obtained, respectively (Table 1). In Table 1, E_{vb} is the vibration energy produced by the explosion load, and E_{vt} is the vibration energy induced by the excavation unloading.

In the practical engineering, rock masses are often in the condition of the nonhydrostatic stress field with the irregular excavation boundary. The solution of strain energy U of the excavated rock masses is not as easy as that of the circular cavity excavation, which needs to be achieved by the numerical simulation method. According to the blasting design in Figure 2 and blasting design parameters of diversion tunnel #4, the blasting excavation calculation model of #4 diversion tunnel was built in ANSYS, as shown in Figure 8. The size of the model is 163 m × 103 m × 80 m

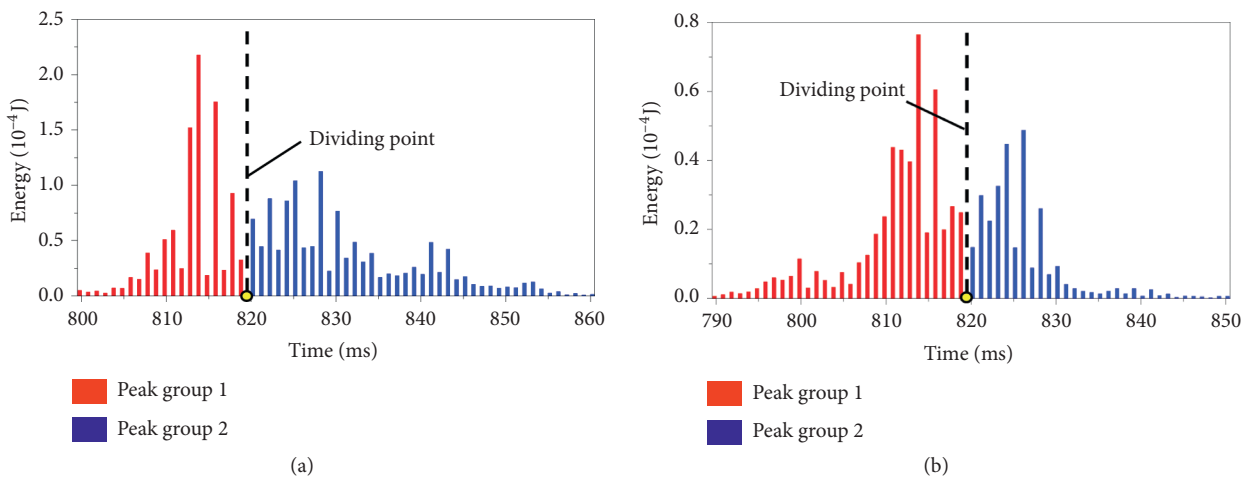

Figure 5: Time-energy density distribution histograms of the monitored vibration in vertical. (a) Monitoring point #2 (MS13). (b) Monitoring point #2 (MS13).

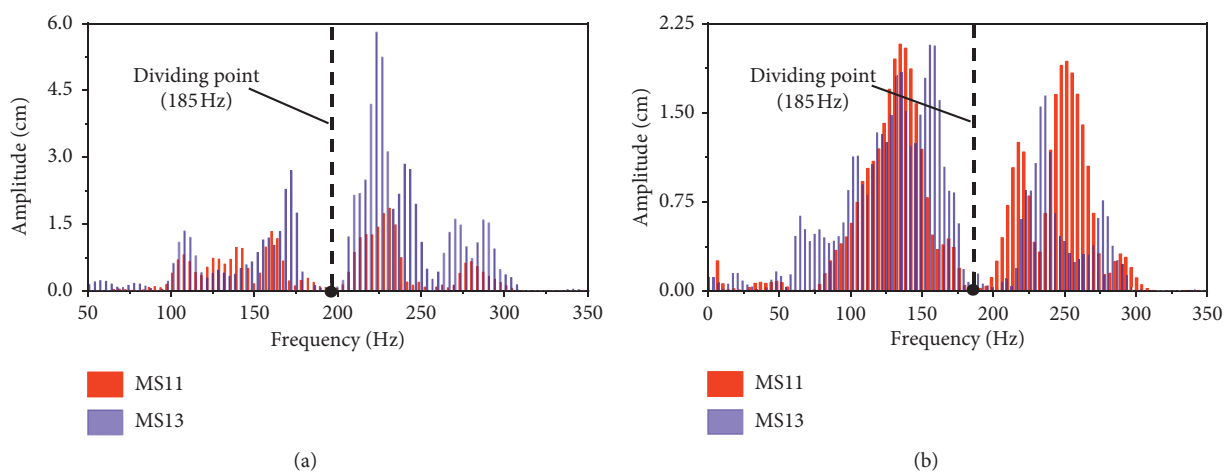

Figure 6: Amplitude spectrums of the monitored vibration waveforms. (a) Monitoring point #2. (b) Monitoring point #3.

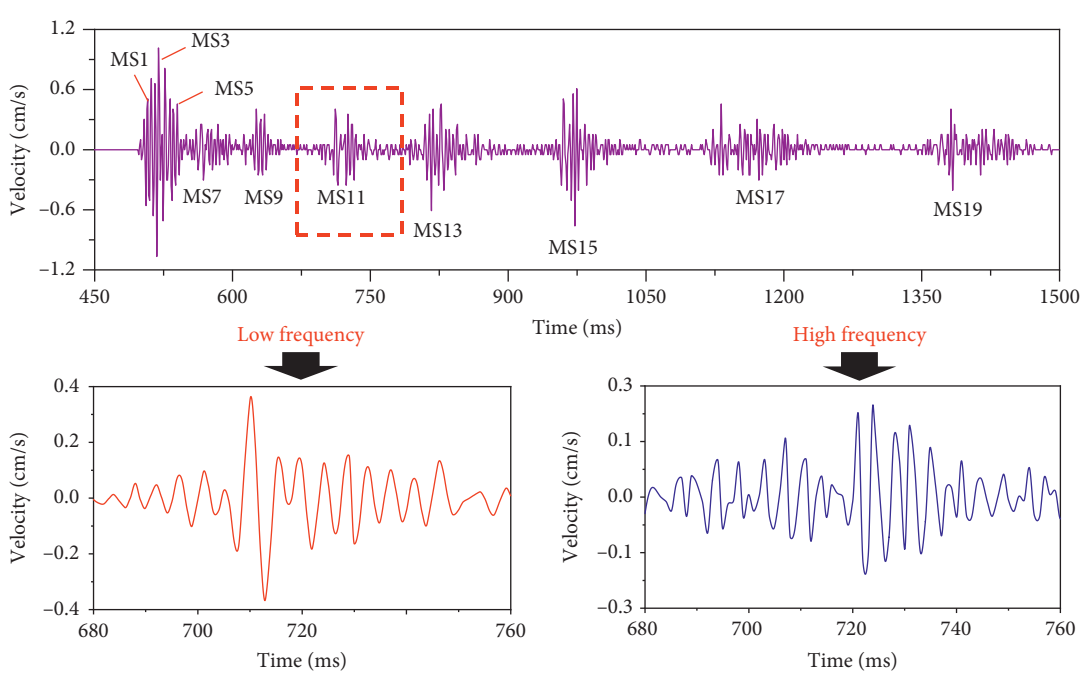

Figure 7: Filtering results of the monitored vibration waveform for MS11.

Table 1: Energy distribution of monitored vibrations and energy of calculation results.

Delay	r (m)	Q (kg)	V (m^3)	E_{vb} (kJ)	E_{vt} (kJ)	U (kJ)	E_E (kJ)
MS1	26.1	30.0	25.6	32	67	1028	79710
MS3	26.1	60.2	23.0	64	59	1181	159951
MS5	26.2	24.0	17.4	35	51	873	63768
MS7	26.2	40.0	26.2	46	70	1276	106280
MS9	26.8	36.0	22.5	38	72	1290	95652
MS11	26.3	40.0	29.5	67	91	1842	106280
MS13	26.4	32.0	22.8	52	83	1681	85024
MS15	27.0	96.0	65.0	142	193	4401	255072
MS17	27.4	39.6	61.9	56	202	4489	105217
MS19	25.6	39.1	45.9	62	84	1528	103888

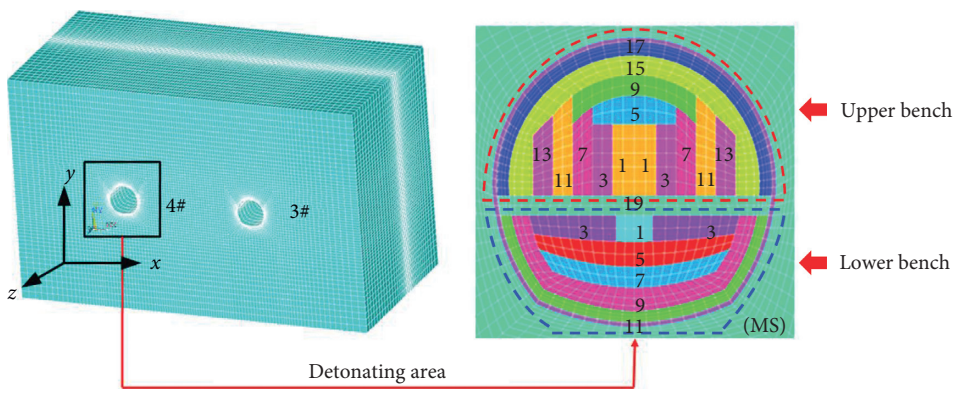

Figure 8: Calculation model.

(length × height × width), and it contains 379728 units. Then, the secondary stress state of the blasting area before the detonation of blast holes for per delay was calculated using the parameters in Table 2 so as to obtain the strain energy U of the excavated rock mass after detonation of blast holes of per delay for upper bench of diversion tunnel #4.

The calculation results of the strain energy U of the excavated rock mass corresponding to the detonation of blast holes for per delay are shown in Table 1. According to the energy of vibration caused by excavation unloading and the strain energy U of the excavated rock mass for the detonation of blast holes of per delay, the coefficient K_1 in equation (24) can be obtained, which is shown in Figure 9.

The explosion heat of $\varphi 32$ emulsion explosives W is 2657 kJ/kg (explosive density: 1100 kg/m^3, detonation wave velocity: 4000 m/s) and the longitudinal wave velocity CL is 4500 m/s, $t_d = 4$ ms. Then, the total energy E_E produced by the explosive during the detonation of blast holes for per delay can be calculated according to the single explosive quantity. Then, the coefficient (η%) in equation (24) can be calculated in combination with the calculated vibration energy of the explosion load (Figure 9). The x-coordinate avg in Figure 9 is the average value of η and K_1, respectively.

According to other data collected from the upper bench of the tunnel: the excavated rock mass volume V, the distance from the blasting center r, and the monitored vibration peak PPV (due to the serious superposition of MS1, MS3, and MS5, they were ignored during the attenuation law analysis), the prediction model proposed in this paper was trained by the multiple regression analysis method, so as to obtain the coefficients K_3 and β in equation (32). To facilitate multiple regression analysis, logarithmic transformation is performed on equation (32):

$$\ln \mathrm{PPV} - \frac{1}{2}\ln\left(\frac{E_t}{\rho V}\right) = \ln K_3 + \beta \ln\left(\frac{V^{1/3}}{r}\right). \tag{38}$$

Order: $x_1 = \ln(V^{1/3}/r)$, $y_1 = \ln \mathrm{PPV} - ((1/2)\, lnt\, (E_t/\rho V))$.

The coefficients K_3 and β in equation (32) can be obtained by the linear fitting of two sets of data x and y. The linear fitting results are shown in Figure 10, where R is the correlation coefficient of fitting. For the convenience of comparison, Figure 10 also shows the linear fitting results using Sadov's empirical formula (equation (39)) and the formula recommended by the United States Bureau of Mines (equation (40)) (in the equations, K_4, α, K_5, and ξ are the coefficients related to the blasting environment).

$$\mathrm{PPV} = K_4\left(\frac{Q^{1/3}}{r}\right)^{\alpha}, \tag{39}$$

$$\mathrm{PPV} = K_5\left(\frac{Q^{1/2}}{r}\right)^{\xi}. \tag{40}$$

As shown in Figure 10, x_2 and y_2 were obtained by logarithmic transformation of equation (39), and $x_2 = \ln(Q^{1/3}/r)$, $y_2 = \ln \mathrm{PPV}$; x_3 and y_3 were obtained by

Table 2: Mechanical parameters.

σ_{xx} (MPa): in horizontal (X-direction)	σ_{yy} (MPa): in vertical (Y-direction)	σ_{zz} (MPa): in tunnel axial (Z-direction)	E_0 (GPa)	μ	ρ (kg/m^3)
49.2	56.9	40.1	56.2	0.25	2700

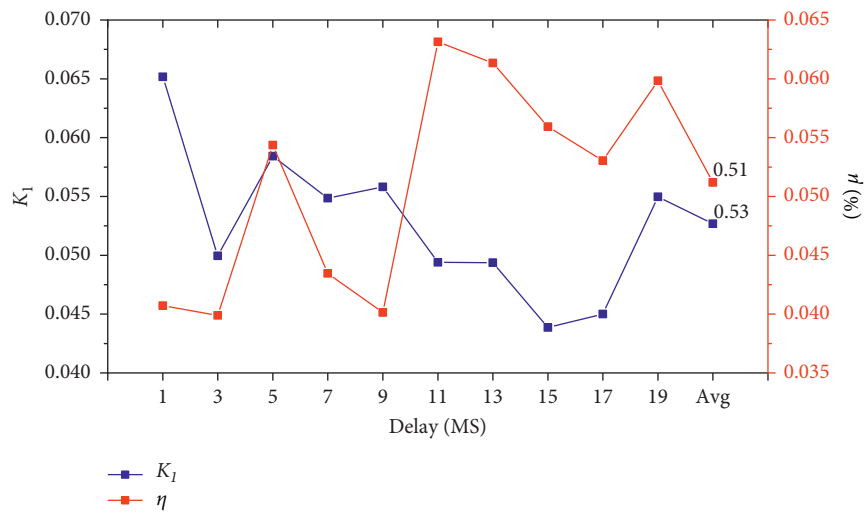

Figure 9: K1 and η.

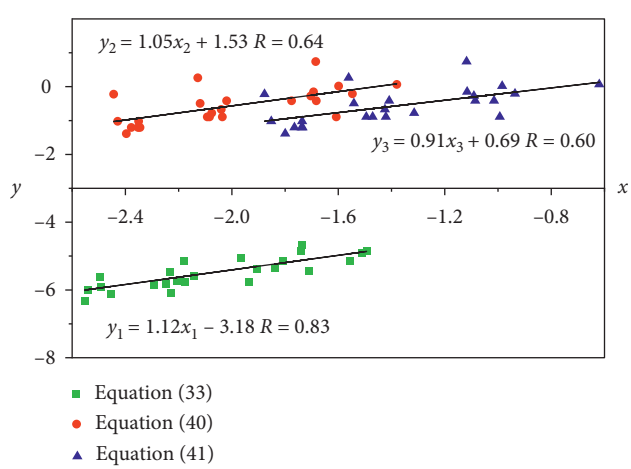

Figure 10: Fitting results of the attenuation law of vibration peak in longitudinal.

logarithmic transformation of equation (40), and $x_3 = \ln(Q^{1/3}/r)$, $y_3 = \ln \mathrm{PPV}$.

According to the fitting results in Figure 10, the unknown coefficients in the equations (32), (39), and (40) are obtained (Table 3). As can be seen from Table 3, the attenuation coefficient of the prediction formula proposed in this paper is basically consistent with that of Sadov's empirical formula, and the accuracy of the fitting correlation coefficient is significantly higher than that of the traditional formula, which indicates that the model proposed in this paper can more accurately predict the vibration induced by the blasting excavation of deep rock mass.

4.4. Testing of Prediction Models. Because the blast holes and charge parameters of the upper and lower benches for the tunnel are similar, the in situ stress and the rock mass quality are consistent. Thus, the prediction formula trained by using the monitored data of the upper bench of the tunnel can be used to predict the vibration induced by blasting excavation of the lower bench of the tunnel. Combined with the data collected from the blasting excavation of the lower bench of tunnel: the volume V of the excavated rock masses, the distance from the blasting center r, the single explosive charge Q, and the strain energy U of the excavated rock mass, the trained formula in Table 3 was used for prediction, and the results were compared with the monitored results. The comparison results between the prediction in longitudinal PPV and the monitored PPV are shown in Figure 11.

In order to better compare several prediction models, the root-mean-square error (RMSE) calculated by the following equation is shown in Table 4.

$$\mathrm{RMSE} = \sqrt{\frac{\sum_1^N (P_i - T_i)^2}{N}}, \tag{41}$$

where P_i, T_i, and N are the predicted PPV, the monitored PPV, and the sample number, respectively. Here, $N = 18$, ($i = 1$–18).

As can be seen from Table 4, the RMSE of the prediction model in this paper is the minimum. Therefore, the model proposed in this paper can be more accurately used to predict the vibration caused by the blasting excavation of the deep rock mass under the high in situ stress.

Table 3: Unknown coefficients and correlation coefficients in equations (32), (39), and (40).

Prediction formula	Coefficient	Longitudinal	Vertical	Horizontal tangential
$\mathrm{PPV} = K_3 (E_t/\rho V)^{1/2} \cdot (V^{1/3}/r)^{\beta}$	K_3	0.042	0.13	0.042
	β	1.12	1.71	1.13
	R	0.83	0.88	0.83
$\mathrm{PPV} = K_4 (Q^{1/3}/r)^{\alpha}$	K_4	4.62	18.14	9.03
	A	1.05	1.76	1.15
	R	0.64	0.81	0.71
$\mathrm{PPV} = K_5 (Q^{1/2}/r)^{\xi}$	K_5	1.99	4.78	3.91
	Ξ	0.91	1.58	1.06
	R	0.60	0.78	0.70

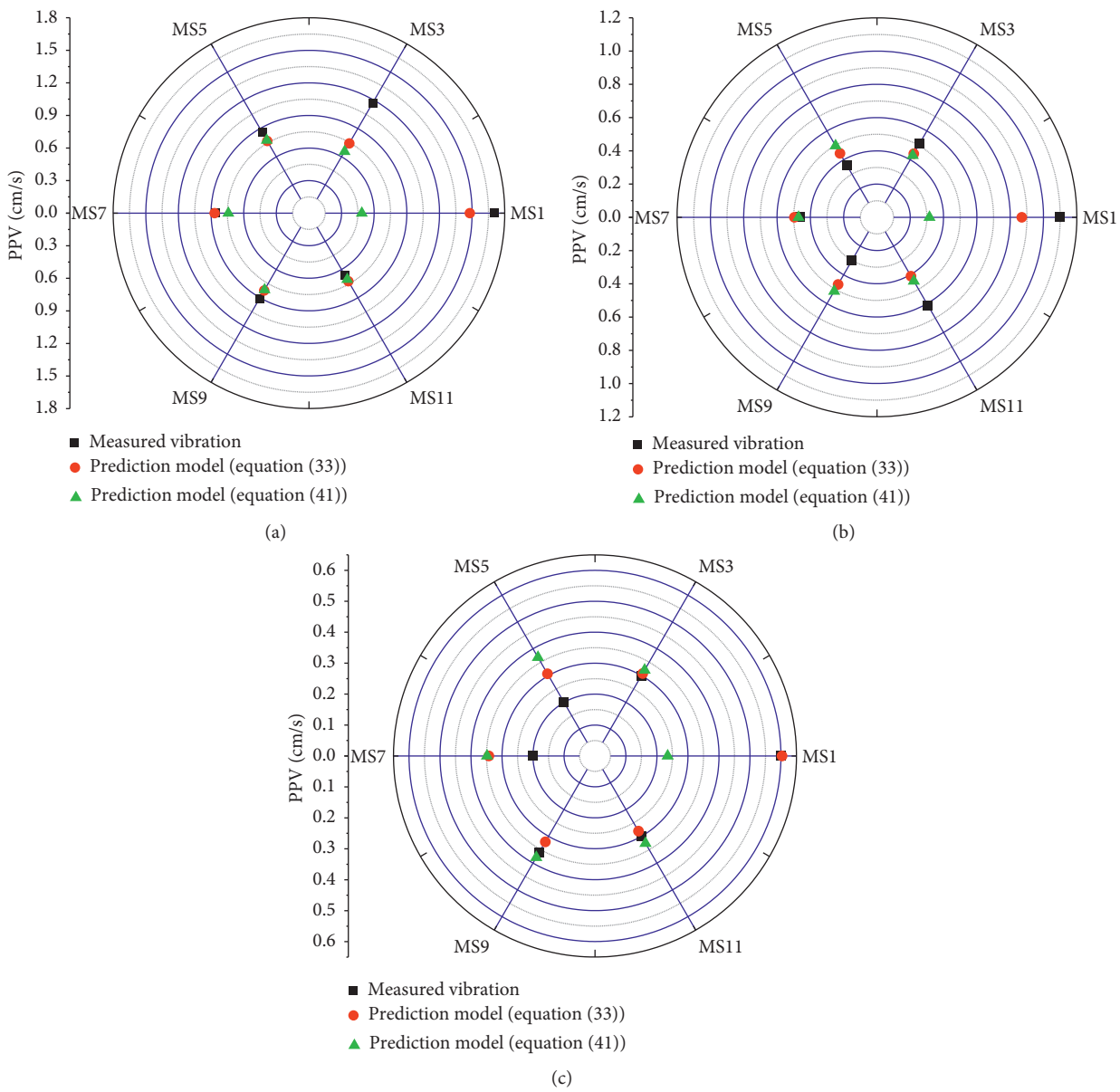

Figure 11: Comparison of predicted vibration and monitored vibration (in longitudinal). (a) Monitoring point #1. (b) Monitoring point #2. (c) Monitoring point #3.

Table 4: Root-mean-square error (RMSE) of the prediction.

Prediction model	RMSE		
	Longitudinal	Vertical radial	Horizontal tangential
Prediction model of equation (32)	0.15	0.26	0.19
Prediction model of equation (39)	0.24	0.33	0.40
Prediction model of equation (40)	0.38	0.39	0.43

5. Conclusions

In the process of deep rock blasting excavation under high in situ stress, the vibration caused by the strain energy release of the rock mass accounts for a considerable proportion in the whole vibration induced by blasting excavation, and the strain energy release of the rock mass and the energy produced by explosive explosion together constitute the energy source of vibration. On this basis, this paper proposed a prediction model of vibration peak for blasting excavation, which takes into account the strain energy release of the rock mass and is applicable for high in situ stress condition. Compared with the prediction model in article [25], the prediction model proposed in this paper is not only applicable for the vibration prediction of excavation in the hydrostatic stress field but also suitable for excavation vibration prediction in nonhydrostatic stress field. Moreover, this prediction model is not limited to a simple excavation profile, and it also has higher accuracy for a more complex excavation profile. In addition, compared with the traditional prediction model mentioned in this paper, the proposed prediction model not only considers the explosive energy but also takes into account the factor of strain energy release of the rock mass during blasting excavation under high in situ stress condition. Finally, according to the testing data, the model has higher fitting correlation coefficient and lower root-mean-square error (RMSE) of the prediction and can more accurately predict the vibration peak of blasting excavation under high in situ stress condition for relatively complex working conditions.

Data Availability

Previously reported [28] data were used to support this study and are available at DOI: 10.1201/9781439833476.ch36.

Conflicts of Interest

The authors declare that there are no conflicts of interest regarding the publication of this paper.

Acknowledgments

This work was supported by the National Natural Science Foundation of China (51979152), Educational Commission of Hubei Province of China (T2020005), Open Foundation of Hydraulic Rock Mechanics of Ministry of Education (RMHSE1603), and Open Foundation of Hubei Key Laboratory of Construction and Management in Hydropower Engineering (2016KSD11). The authors would like to thank all the supporters.

References

[1] H. T. Zhao, K. D. Jiang, R. Yang, Y. Tang, and J. Liu, "Experimental and theoretical analysis on coupled effect of hydration, temperature and humidity in early-age cement-based materials," *International Journal of Heat and Mass Transfer*, vol. 146, Article ID 118784, 2020.

[2] M. C. He, H. P. Xie, S. P. Peng, and Y. D. Jiang, "Study on rock mechanics in deep mining engineering," *Chinese Journal of Rock Mechanics and Engineering*, vol. 24, no. 16, pp. 2803–2813, 2005.

[3] M. Y. Wang, Z. P. Zhou, and Q. H. Qian, "Tectonic, deformation and failure problems of deep rock mass," *Chinese Journal of Rock Mechanics and Engineering*, vol. 25, no. 3, pp. 448–455, 2006.

[4] T. Rabczuk and T. Belytschko, "A three-dimensional large deformation meshfree method for arbitrary evolving cracks," *Computer Methods in Applied Mechanics and Engineering*, vol. 196, no. 29-30, pp. 2777–2799, 2007.

[5] T. Rabczuk, R. Gracie, J. H. Song, and T. Belytschko, "Immersed particle method for fluid–structure interaction," *International Journal for Numerical Methods in Numerical Methods in Engineering*, vol. 81, no. 1, pp. 48–71, 2010.

[6] T. Rabczuk, G. Zi, S. Bordas, and N. X. Hung, "A simple and robust three-dimensional cracking-particle method without enrichment," *Computer Methods in Applied Mechanics and Engineering*, vol. 199, no. 37–40, pp. 2437–2455, 2010.

[7] M. Khandelwal and T. N. Singh, "Prediction of blast-induced ground vibration using artificial neural network," *International Journal of Rock Mechanics and Mining Sciences*, vol. 46, no. 7, pp. 1214–1222, 2009.

[8] H. Dehghani and M. Ataee-pour, "Development of a model to predict peak particle velocity in a blasting operation," *International Journal of Rock Mechanics and Mining Sciences*, vol. 48, no. 1, pp. 51–58, 2011.

[9] M. Kamali and M. Ataei, "Prediction of blast induced vibrations in the structures of Karoun III power plant and dam," *Journal of Vibration and Control*, vol. 17, no. 4, pp. 541–548, 2011.

[10] M. Mohamadnejad, R. Gholami, A. Ramezanzadeh, and M. E. Jalali, "Prediction of blast-induced vibrations in limestone quarries using support vector machine," *Journal of Vibration and Control*, vol. 18, no. 9, pp. 1322–1329, 2012.

[11] M. Cardu, D. Coragliotto, and P. Oreste, "Analysis of predictor equations for determining the blast-induced vibration in rock blasting," *International Journal of Mining Science and Technology*, vol. 29, no. 6, pp. 905–915, 2019.

[12] S. R. Dindarloo, "Prediction of blast-induced ground vibrations via genetic programming," *International Journal of Mining Science and Technology*, vol. 25, no. 6, pp. 143–147, 2015.

[13] M. Cardu, M. Dompieri, and J. Seccatore, "Complexity analysis of blast-induced vibrations in underground mining: a case study," *International Journal of Mining Science and Technology*, vol. 22, no. 1, pp. 125–131, 2012.

[14] Standards of the People's Republic of China, *GB6722-2014: Safety Regulations for Blasting*, China Standard Press, Beijing, China, 2014.
[15] L. Xibing and G. Desheng, *Rock Impact Dynamics*, Central South University of Technology Press, Changsha, China, 1994.
[16] W. Zhao, *Rock Mechanics*, Central South University Press, Changsha, China, 2010.
[17] H. Guozhong, H. Wang, X. Li et al., "Research on blasting vibration regularity of bedrock digging of embankment project," *Rock and Soil Mechanics*, vol. S2, pp. 1036–1040, 2006.
[18] W. Lu, J. Yang, P. Yan et al., "Dynamic response of rock mass induced by the transient release of in-situ stress," *International Journal of Rock Mechanics and Mining Sciences*, vol. 53, no. 9, pp. 129–141, 2012.
[19] J. Yang, W. Lu, M. Chen, P. Yan, and C. Zhou, "Microseism induced by transient release of in situ stress during deep rock mass excavation by blasting," *Rock Mechanics and Rock Engineering*, vol. 46, no. 4, pp. 859–875, 2013.
[20] J. Yang, W. Lu, Q. Jiang, C. Yao, S. Jiang, and L. Tian, "A study on the vibration frequency of blasting excavation in highly stressed rock masses," *Rock Mechanics and Rock Engineering*, vol. 49, no. 7, pp. 2825–2843, 2016.
[21] M. N. Toksöz and H. H. Kehrer, "Tectonic strain release by underground nuclear explosions and its effect on seismic discrimination," *Geophysical Journal Royal Astronomical Society*, vol. 31, no. 1–3, pp. 141–161, 1972.
[22] R. P. Young, S. Talebi, D. A. Hutchins, and T. I. Urbancic, "Analysis of mining-induced microseismic events at Strathcona mine, Sudbury, Canada," *Pure and Applied Geophysics*, vol. 129, no. 3-4, pp. 455–474, 1989.
[23] R. P. Young and S. C. Maxwell, "Seismic characterization of a highly stressed rock mass using tomographic imaging and induced seismicity," *Journal of Geophysical Research: Solid Earth*, vol. 97, no. B9, pp. 361–373, 1992.
[24] P. Yan, W. B. Lu, M. Chen, and C. Zhou, "Study on impaction of initial geostress field on vibration of surrounding rock during excavation with drilling and blasting method," *Chinese Journal of Rock Mechanics and Engineering*, vol. 27, no. 5, pp. 1036–1045, 2008.
[25] P. Yan, W. B. Lu, and C. B. Zhou, "Research on vibration induced by dynamic unloading of in-situ stress in asymmetrical geostress field," *Chinese Journal of Rock Mechanics and Engineering*, vol. 27, no. 4, pp. 773–781, 2008.
[26] J. A. Sanchidrian, P. Segarra, and L. M. López, "Energy components in rock blasting," *International Journal of Rock Mechanics and Mining Sciences*, vol. 44, no. 1, pp. 130–147, 2007.
[27] M. D. G. Salamon, "Energy considerations in rock mechanics: fundamental results," *Journal of the South African Institute of Mining and Metallurgy*, vol. 84, no. 8, pp. 233–246, 1984.
[28] W. B. Lu and W. Hustrulid, "The Lu-Hustrulid approach for calculating the peak particle velocity caused by blasting," in *Proceeding of the 2nd World Comference on Explosive and Blasting Technique*, pp. 291–300, Praque, Czech Republic, September 2003.